The reproducibility of passive human knee-joint motion characteristics

42. THE REPRODUCIBILITY OF PASSIVE HUMAN KNEE-JOINT MOTION CHARACTERISTICS

L. Blankevoort, R. Huiskes and A. de Lange

Laboratory for Experimental Orthopaedics, University of Nijmegen, Nijmegen, The Netherlands

1. INTRODUCTION

The human knee-joint is a complex kinematic system for which a coherent quantitative functional description is not available yet, despite a relatively large amount of experimental kinematic data, presented in the literature. The quantitative variety among the literature data is caused by differences in accuracies of the several methods applied, but may as well be a result of interindividual differences among knee-joint specimens.

The general objective of the present investigation is the validation and development of a mathematical knee-joint model to describe 3-D passive kinematics. The approach is to obtain accurate and complete kinematic descriptions of knee-joint behavior in an adequate number of specimens with a variety of external loading configurations, and to simulate this behavior in a mathematical model, thereby optimizing the model characteristics to obtain adequate agreement in individual cases.

The most important properties of the knee, as for instance joint surface geometry and ligament configurations are measured in the experimental specimen and used as input parameters of the model. Once the model is validated, it can be applied for extensive parametric analyses to investigate the significance of joint structures, the effects of lesions and the consequences of surgical interventions.

The theoretical and numerical formulations of the mathematical model used in this case has been published earlier (1,2). The present paper reports purely on the accuracy of the kinematic experiments and the reproducibility of the experimentally obtained passive knee-joint motion characteristics.

2. METHODS

The freshly frozen intact knee-joint specimens are clamped into a knee-loading apparatus in which the flexion angle can be prescribed. The other degrees of freedom-of-motion are left free for the tibia to find its equilibrium position at each flexion step, while moderate tibial rotation torques (M_y), axial forces (F_y) and A-P forces (F_z) can be applied (Fig.1).

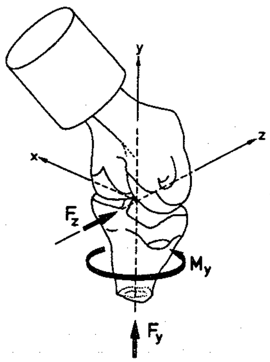

FIGURE 1. The tibial coordinate system and the loads that can be applied.

The actual spatial positions of the tibia and the femur after each motion step are determined with use of a Roentgenstereophotogrammetric system (3). Up to six tantalum pellets, 0.8 mm in diameter, are inserted in femur and tibia. At each flexion position two Roentgen exposures are made, which are later evaluated on a 2-D coordinate digitizer. A computer program reconstructs the 3-D coordinates of the pellets with respect to the laboratory coordinate system. A subsequent computer program calculates the motion characteristics of the tibia with respect to femur (or vice versa) in terms of three Euler rotations and three translations.

The rotations are expressed as occurring around the coordinate axes of the tibia (Fig.1), in the sequence flexion (around the x-axis), tibial rotation (y-axis), and approximate ad/abduction rotation (z-axis). The tibial origin is located in the posterior apex of the anterior cruciate ligament insertion region on the tibial plateau.

In addition, finite helical axes are calculated for each motion step (4). These are represented in the tibial coordinate system, as if the femur was moving with respect to a fixed tibia.

The accuracy of the experimental method is determined in two ways. First the stereo-Roentgenograms of one experiment are re-evaluated and the motion pathway reconstructed. Consequently two sets of values of the kinematic parameters for each flexion step are obtained and are used to calculate the standard deviation for each parameter according to (5):

$$S_d = \sqrt{\frac{\sum_{i=1}^{n} (P_{i1} - P_{i2})^2}{2n}}$$

in which

S_d = Standard deviation of a kinematic parameter
P_{i1} = Result of first reconstruction
P_{i2} = Result of second reconstruction
n = Number of duplicate values

Secondly a specific experiment is repeated. The standard deviations are calculated in the same way.

Because the knee-joint does not have precise anatomic landmarks, differences occur in the alignments of the specimens in the laboratory reference system. This influences the calculated values of the Euler rotations. To estimate the quality of this effect, specific motion patterns of one specimen are re-calculated, using alternative reference systems.

3. RESULTS

Four specimen (21 through 24) were used, of which two were bilateral (23 and 24). The tests were performed on the intact knees, using several different combinations of external loads. Only some results, related to the accuracy and reproducibility of the tests, will be presented here (6).

The exo- and endorotation motion pathways of the four specimens as functions of the flexion angle are shown in Fig.2.a. The ad/abduction rotation, which is coupled with the flexion motion, is represented in Fig.2.b. While the shape of the exo/endorotation curves of the different specimens is remarkably similar, that of the ad/abduction curves is not. But evidently, the tibia is more in abduction during the endorotation pathway than during the exorotation pathway.

To illustrate the significance of these motion pathways, the standard deviations of the Euler rotations are given in Table 1, for the repeated reconstruction, and in Table 2 for the repeated experiment.

The effect of alignment of the specimens relative to the laboratory reference system is shown in Fig.3. In this the reference system is rotated plus and minus 5 degrees, and new Euler rotations are calculated. Evidently some of the differences apparent in Fig.2 are reproduced here. Hence, the differences in the behavior of the separate specimens are probably partly due to alignment effects.

The helical axes of the exorotation pathway of one specimen are represented in Fig.4, in a frontal view and as piercing points (intersections) with two sagittal planes. The numbers indicate the subsequent flexion steps for which the helical axes are calculated. The oblique position of the first axis is caused by the considerable amount of tibial exorotation in the first flexionstep. In Fig.5 the same phenomena can be noticed in case of an endorotation pathway. In Fig.6 the piercing points with the two sagittal planes of the four specimens are shown for an endorotation motion pathway. The patterns of the piercing points are very similar. The same degree of similarity of the helical axis patterns is found for the exorotation pathway.

Table 1. Repeated reconstruction.
Standard deviation of Euler Rotations

	spec.23 (n=13)	spec.24 (n=14)
Flexion (degrees)	0.09	0.07
Endo/exorotation "	0.07	0.07
ad/abduction "	0.06	0.07

Table 2. Repeated experiment.
standard deviation of Euler Rotations

	spec.23 (n=13)	spec.24 (n=14
Flexion (degrees)	0.1	0.2
Endo/exorotation "	0.2	0.3
ad/abduction "	0.2	0.4

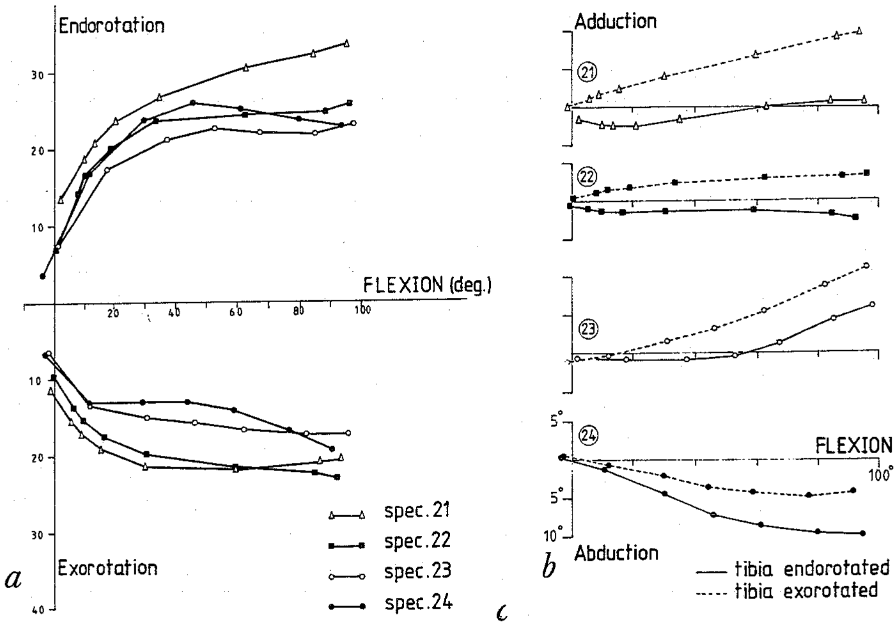

FIGURE 2. a) The endorotation (M_y = 3 Nm) and the exorotation (M_y = -3 Nm) motion pathways of four specimen (F_y = 150 N). **b)** Ad- and abduction rotations for the same motion pathways.

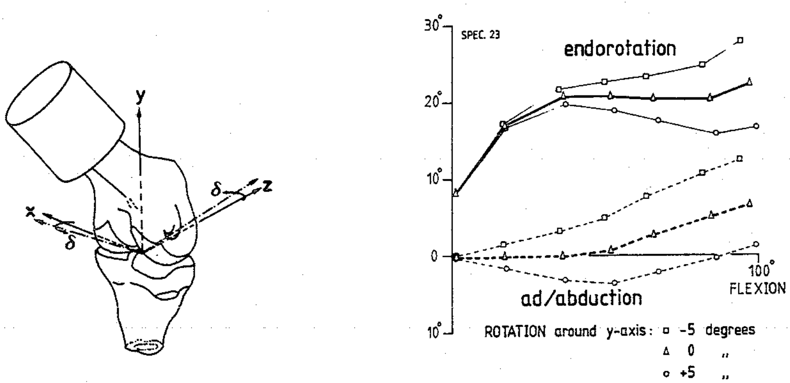

FIGURE 3. Endorotation and ad/abduction curves re-calculated with respect to three alternative reference systems rotated -5,0 and +5 degrees around the y-axis (specimen 23, F_y = 0 N, My = +3 Nm).

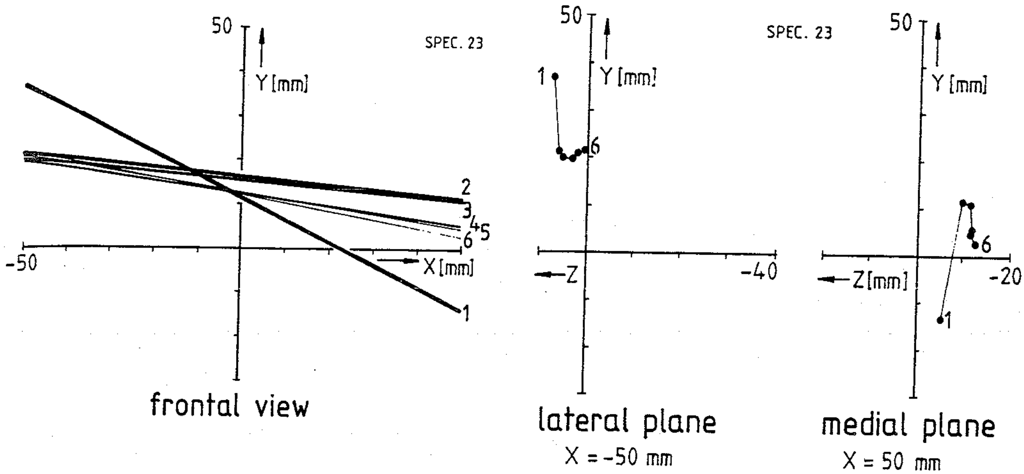

FIGURE 4. Frontal view of the helical axes of specimen 23 for an exorotation motion pathway and the piercing points of the axes with two sagittal planes. (F_Y = 150 Nm, M_Y = -3 Nm, 1: -2-12, 2: 12-31, 3: 31-46, 4: 46-62, 5: 62-82, 6: 82-96 degrees flexion).

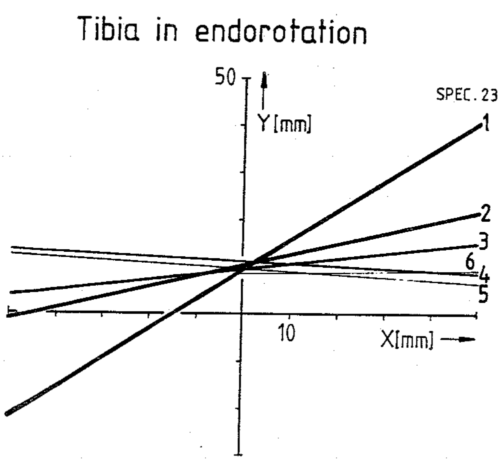

FIGURE 5. Frontal view of the helical axes of specimen 23 for an endorotation motion pathway (F_Y = 150 N, M_Y = 3 Nm, 1: 1-18, 2: 18-37, 3: 37-53, 4: 53-67, 5: 67-85, 6: 85-98 degrees flexion).

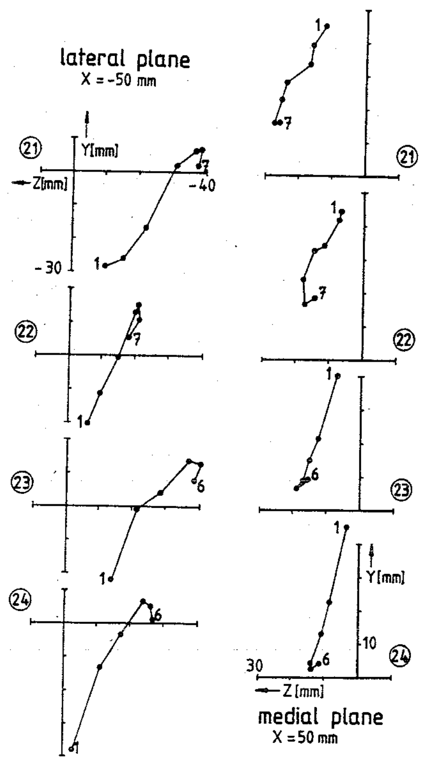

FIGURE 6. Piercing points of the helical axes with two sagittal planes of four specimen for an endorotation motion pathway (F_Y= 150 N, M_Y = 3 Nm).

4. DISCUSSION

Accurate kinematic characteristics of four knee-joint specimens in a variety of moderate external loading configurations are obtained. Together with geometric data, these findings can be used as a database for verifying and enhancing existing knee-joint models. With respect to the reproducibility of knee-joint motion characteristics some conclusions can be made.

The exo- and endorotation curves in Fig.2.a represent the limits of the tibial rotation freedom-of-motion. When no tibial torque is applied, the joint may follow an arbitrary motion pathway within these limits. This is one of the causes for controversies in the literature where knee motion patterns are concerned.

We found reproducible kinematic data for the specific exo- and endorotation pathways of four specimens. In particular the finite helical axes (Fig.6) are unique in their reproducibility as compared to others in the literature (e.g. 7). When kinematic data are represented in terms of Euler rotations, the differences that do occur can partly be explained by different alignments of the specimens relative to the laboratory reference system (Fig.3). The helical axes are not susceptible to alignment differences, only their representation with respect to a coordinate system is. Therefor they are helpful when comparing kinematic characteristics of different knee-joint specimens with each other, or with those of kinematic knee-joint models.

REFERENCES

1. Wismans J, Veldpaus F, Janssen J, Huson A, and Struben P. 1980. A three-dimensional mathematical model of the knee-joint. J.Biomech. 13, 677-685.
2. Dortmans L, Sauren A, Veldpaus F, Huson A. 1984. A simplified quasi-static model of the human knee-joint based on a general two-body-system theory. 4th Meeting European Society of Biomechanics, Davos, Switzerland.
3. De Lange A, van Dijk R, Huiskes R, Selvik G, and van Rens ThJG. 1982. The application of Roentgenstereophotogrammetry for evaluation of knee-joint kinematics in vitro. In: Biomechanics: Principles and Applications (R Huiskes et al, Eds) Martinus Nijhoff Publ, 177-184.
4. Goldstein H. 1959. Classical Mechanics. Addison-Verlag, Reading, M.A.
5. Mikhail EM. 1976. Observations and Least Squares. New York, IEP-1 Dun-Donnelley.
6. Blankevoort L, Huiskes R, de Lange A. 1984. An in-vitro study of the passive kinematic behavior of the human knee-joint. Proc. ASME Winter Annual Meeting, Bioengineering Symposium, New Orleans (LA), USA.
7. Blacharski PA, Somerset JH, and Murray DG. 1975. A three-dimensional study of the kinematics of the human knee. J.Biomech. 8, 375-384

ACKNOWLEDGEMENTS: This research is performed in co-operation with the Dept. of Mechanical Engineering of the Eindhoven Univ. of Technology, The Netherlands and the Univ. of Lund, Sweden, and is sponsored by Grant 90-90 of the Netherlands Organization for the Advancement of Pure Research (ZWO).